Modeling and Analysis of 5 Axis Milling Configurations and Titanium Alloy Surface Topography

David PRAT[1]
Arts et Metiers ParisTech
LaBoMaP, Rue Porte de Paris, Cluny 71250, FRANCE
david.prat@ensam.eu

Guillaume FROMENTIN
Arts et Metiers ParisTech
LaBoMaP, Rue Porte de Paris, Cluny 71250, FRANCE
guillaume.fromentin@ensam.eu
ASME Membership

Gérard POULACHON
Arts et Metiers ParisTech
LaBoMaP, Rue Porte de Paris, Cluny 71250, FRANCE
gerard.poulachon@ensam.eu

Emmanuel DUC
IFMA/UBP
Institut Pascal, Campus des Cézeaux BP265-63175 Aubière cedex, FRANCE
emmanuel.duc@ifma.fr

ABSTRACT

5-axis milling with a ball end cutter is commonly used to generate a good surface finish on complex parts, such as blades or impellers made of titanium alloy. The 5-axis milling cutting process is not straight forward; local cutting conditions depend a lot on the geometrical configuration relating to lead and tilt angles. Furthermore, the surface quality is greatly affected by the cutting conditions that define the milling configuration. This study presents a geometrical model of 5-axis milling in order to determine the effective cutting conditions, the milling mode, and the cutter location point. Subsequently, an analysis of surface topography is proposed by using the geometrical model, local criteria, and a Principle Component Analysis

[1] Corresponding author.

of experimental data. The results show the effects of local parameters on the surface roughness, in relation to the lead and tilt angles.

KEYWORDS
5-axis milling, titanium alloy, surface topography, effective diameter, milling mode

INTRODUCTION

The present study deals with the surface topography obtained through 5-axis milling of a titanium alloy. The finish quality depends mainly on the tool geometry, the cutter location point and the cutting conditions. For a ball end mill, the cutting speed is variable along the cutting edge because effective cutting diameters are not constant. Furthermore, for a cutter with 4 teeth or more, the number of working teeth, i.e. really involved in the cutting operation, is a function of the axial and radial depth of cut and the tool inclination. As a consequence, the local surface machining obtained by 5 axis point milling is not simply estimated. It is necessary to propose a geometrical cutting model to perform adequate local cutting conditions and evaluate the local surface roughness. The aim of this article and its originality is to provide an analytical model for the computation of local parameters in 5-axis milling and to establish the connections between these local cutting conditions and the measured surface topography with the use of a Principle Component Analysis. The proposition of a new, original and more complex model ensures a more accurate study of the local surface topography.

Titanium alloys are commonly used in aeronautic and aerospace industrial sectors [1] and are also known for having a low machinability. Generally part requirements impose a severe quality standard for the surface roughness, whereas the machinability of the titanium alloys and the free form shape to be machined introduce

perturbations on the roughness. To improve the control of the surface roughness, it is necessary to propose an approach that permits the evaluation of the local effective cutting conditions and the associated local surface topography.

Cutting conditions, and especially the cutting speed, play an important role on the tool wear [2] and the surface quality. For a ball end mill, cutting speed varies along the cutting edge. Using the spindle speed and the effective cutting diameters, some studies propose numerical models based on effective cutting diameters to calculate the cutting speed. The main problem is then to evaluate the effective cutting diameters at each position of the machining tool path. This diameter is dependent on the characteristics of the tool, the surface geometry, the cutting conditions and the tool orientation as shown in Fig. 1. Kim et al. [3] propose an initial numerical approach calculation based on a linear tool path. More recently, Fan [4] computes the cutting speed through polynomial interpolation trajectories on 3-axis milling machines.

Other models are proposed in [5,6]. These analytical models consider that the effective diameters are located in the same plane defined by the vector of the outward normal of the finished surface and the tool axis vector. However, this assumption is too broad for any 5-axis milling configuration because it depends on the tool inclination angle as shown in Fig.1. Ozturk and Lazoglu [7] propose an analytical modeling of the tool engagement for 4-axis point milling, but without calculating the effective diameters. Our previous study [8] presents an analytical modeling of the effective diameters and experimental tests to validate the calculation method and assumptions. However this study does not establish links between modeling and cutting phenomena

including the surface quality. In particular, this model does not take into account the number of working teeth and the milling mode. Thus, in the case of the ball end cutter, we consider that the literature does not propose a general analytical modeling of the geometrical problem and consequently the relation between the local cutting conditions and the surface topography.

Concerning the surface topography, several analytical and numerical methods are proposed in the literature. Analytical approaches are limited to characterizing the scallop height as a function of cutting conditions and the tool geometry as [9]. Lin and Koren [10] provide a modeling of the scallop height with consideration of the curvature of the complex surface. Nonetheless, these approaches do not propose accurate models of the surface topography in the feed direction. From this point of view, the numerical approaches are more suitable. Using a series of Boolean operations between the envelope volume of the tool path, Imani and Elbestawi [11] and Bailey et al. [12] propose to build the final surface of the part. The basic assumption of these approaches is the perfect cut of the tool, subsequently the surface topography is a result of the successive positions of the cutting edges. Bouzakis et al. [13] determine the material remaining stock on the part by a series of planar discretizations. Another, more common, modeling of the surface topography is based on the buffer method to specify the height of the material remaining on a surface. This model is used for a bull nose end mill [14–16] or a ball end mill [17–19]. Denkena et al. [20] complete this model with a stochastic surface topography contribution. This complement is a model of the

differences between numerical approach and experimental measurements topographies.

The experimental characterization of the surface topography generated with a ball end mill is proposed by several authors. Zhang et al. [21], Han and Zhao [22] and Chen et al. [23] studied the effect of milling with a two teeth tool on amplitude roughness parameters. All studies are carried out with a constant spindle rotation speed but several tool inclinations, which involve a variation of the cutting speed. Then, the interpretation of the results is not obvious and such an approach does not allow for a distinction between the effect of cutting speed and the effect of the tool inclination to be made. Thus, this study will analyze the relations between local cutting conditions and surface topography through experimental tests with the following parameters considered independently as much as possible: the milling mode, the cutting speed and the position of the cutter location point.

Consequently, this study proposes a geometrical model of cutting tool engagement to determine, for any 5 axis configuration, the diameters corresponding to the points of the edge generating the finished surface, and the intersection surface. The paper is organized as follows. The geometrical model of the 5-axis point milling is presented in the 2nd section with the calculation method of the effective cutting diameters, the number of working teeth, and the determination of the milling mode. Afterwards, experimental relationships between local cutting conditions and surface topography are investigated in the 3rd section. Then we propose to use the Principle Component Analysis to correlate the experimental roughness data with the three

influencing parameters: the milling mode, the cutting speed and the position of the cutter location point C_L.

2. Geometrical Model of the 5-axis Milling Operation

The originality of this model is to propose an analytical approach of cutting geometrical phenomena in the case of 5 axis machining. It is considered that the feed movement is negligible with respect to the cutting movement and thus the surface generated by the cutting edge can be modeled based on the tool envelope. Moreover, it is assumed a geometrical tool engagement based on plane straight 5 axis milling paths.

2.1. Parameterization of the Milling Operation

The process coordinate system illustrated in Fig. 2 is defined by the following vectors: feed direction *T*, cross-feed direction *N*, and normal surface direction *Z*. The axis tool orientation is defined by the tilt angle β_n and lead angle β_f. The lead angle β_f is measured between the projection of the axis tool in the plane (*N, Z*) and the normal surface *Z*. The tool axis is noted Z_t.

The envelope of the tool is modeled by a sphere with a radius r_t equal to the tool radius and the point *O* as the centre of the sphere. The point *O* has the coordinate (0, 0, r_t) in the process coordinate system.

The scallop height *Rz* is calculated with the equation 1:

$$Rz = r_t - \sqrt{{r_t}^2 - \frac{{a_r}^2}{4}} \qquad (1)$$

On Fig. 3, the picturing of the color surface is a function of the point position on the *Z* axis. During the process, a point located on the actual tool path in an area outer of the boundary defined by the machined scallop will be cut in the next tool path (represented

by the dark grey level), otherwise this point belongs to the finished surface (lighter grey level).

The geometrical model of the part during milling, Fig. 3, is composed of the actual tool path, several previous tool paths, the cut surface, and finally, the surface to cut (which will be cut in the next path). The cut surface is defined by the surface which is the intersection between the sphere of the tool envelope and the part. Each path generates a cylinder having a r_t radius, and are a distance of the radial depth of cut, a_r, from each other. The radial depth of cut is chosen positive if the previous tool path is positioned in the positive side of the *N* axis. The cut surface is modeled by a sphere portion represented by the white color in Fig. 3. Three curves, *B1*, *B2* and *B3,* are the borders between the cut surface and the surface to cut, the actual tool path and the previous tool path.

2.2. Effective Cutting Diameters

The calculation method of the effective cutting diameters is based on the distance between the tool axis and the intersections of the tool envelop and the part. The main steps of the method are shown in Fig. 4. To obtain the effective diameters, the borders between the sphere of the cut surface and the part have to be modeled. There are 3 borders as shown in Fig. 3 and analytical equations are developed in [8]. The distance between a point *M* of one border and the tool axis (O, Z_t) is calculated by:

$$Distance[M,(O,Z_t)] = \|OM \times Z_t\| \quad (2)$$

In the Eq.2, the symbol × is the cross product between the vector *OM* and Z_t. The maximum effective cutting diameter is determined as twice the maximum of the function *Distance* on the three borders:

$$D_{eff\ max} = 2.R_{eff\ max} = 2.Maximum_i\left[Distance[Bi,(O,Z_t)]\right] \quad (3)$$

The minimum effective cutting diameter is determined as twice the minimum of the function *Distance* on the three borders. However, if the cutter location point is in the cut surface, the minimum effective cutting diameter is equal to zero:

$$D_{eff\ min} = 2.R_{eff\ min} = 2.Minimum_i\left[Distance[Bi,(O,Z_t)]\right] \quad (4)$$

In order to have more information on the milling configuration, the effective cutting diameters can be determined on the finished surface ($D_{eff\ max\ finished\ surf}$ & $D_{eff\ min\ finished\ surf}$), cf. Fig. 1, which allows the range of the cutting speed that machine the finished surface to be known. The finished surface is defined as a small part of the cut surface which is under the boundary of the machined scallop. The evaluation of these two new diameters is done with changing the axial depth of cut a_a equal to the scallop height (Eq.1). The observation on Fig. 1 demonstrates that in the general cases, the effective cutting diameters are not coplanar and therefore cannot be determined with a single cross section.

In conclusion, the proposed analytical model computes the effective cutting diameters (minimum and maximum) of the cut and finished surface for any 5 axis milling configuration for a linear trajectory. The original results shown in this part indicate that the effective cutting diameters are generally not in the same plane.

2.3. Number of Working Teeth

Ball end milling cutters present various geometries, especially with different numbers of teeth, which directly affect the feed rate. For example, the solid carbide ball-end mill used in this study, shown in Fig. 5, has the reference Jabro 160120MEGA-64 and is characterized by r_t = 6 mm and 4 teeth (but only 2 if the tool diameter is under 4.65 mm).

A larger number of teeth increases the feed rate and thus the productivity. However, the grinding of such tools is more complicated, especially if all teeth join the cutter location point C_L. Frequently, like in Fig. 5, only 2 teeth meet the cutter location point C_L and the two others are not complete and located from a diameter equal to *Dz* (4.65 mm in this case) to a $2.r_t$ one. According to the tilt and lead angles, the portion of the cutting edge in contact with the milled surface is determined between the minimum and the maximum effective cutting diameters. This results in three cutting situations:

- $D_{eff\ min} > Dz$, the 4 teeth of the tool are cutting,
- $D_{eff\ max} > Dz > D_{eff\ min}$, the cutting operation involves 4 teeth for effective diameters upper *Dz* and 2 teeth otherwise,
- $D_{eff\ max} < Dz$, only 2 teeth are engaged during milling.

Knowing the number of working teeth is essential to determining the feed rate of the operation. Furthermore, the quality of the surface topography is linked with the feed rate and the real number of teeth in contact with the part. Thus, *Dz* diameter has to be compared with the effective cutting diameters on the finished surface ($D_{eff\ max\ finished\ surf}$ & $D_{eff\ min\ finished\ surf}$), to know if this consideration impacts the surface

topography, as well as compared with the effective cutting diameters on the cut surface, to evaluate more generally if the process is affected.

2.4. Milling Mode

The milling mode is a characteristic of the local process with two main possibilities: the up milling mode and the down milling mode. The mode depends on the geometrical configuration and can be determined by two different approaches. One is the variation of the uncut chip thickness as a function of time (not developed in this study); the other is defined by the sign of the scalar product between the cutting speed V_c and the feed rate V_f. After analyzing this scalar product, it appears that the boundary for which it is null, is a circle characterized by a r_t radius, the centre position is the O point and included in the plane (O,Z_f,T), as shown in Fig. 6. If the material to cut is on the left side (respectively right side) of the (O, Z_f, T) plane in the direction of the feed rate, the scalar product is positive (respectively negative) so the milling mode is up milling (respectively down milling).

In the particular situation of Fig. 6, according to the specific inclination angle and the radial depth of cut values, the cut surface and the finished surface are machined with a down milling mode. In other cases, depending on parameters, several situations can occur:

- the entire cut surface is done with the same mode,
- the entire finished surface is done with the same mode, but not the same as the cut surface,
- the finished surface is generated with both milling modes.

The consequence of the milling mode on the surface topography will be analyzed in the next section.

2.5 Applications to Different 5 Axis Milling Configurations

The calculation method of the effective cutting diameters and the determination of the milling modes are essential process characteristics to precisely define the local cutting conditions. Four situations (Fig. 7) are analyzed in order to explain the influence of the β_n tilt angle on the milling mode.

In 3 axis milling, the milling mode is determined by the position of the raw material (here defined by the sign of the radial depth of cut). In slotting operations, the cutting edge starts to cut with up milling mode and then finishes with the down milling mode.

In the first situation of Fig.7, the raw material is located on the right side (when the tool moves away from the observer) of: the actual tool path (i.e. $a_r > 0$), the normal of the machined surface (O, Z) and the right of the tool axis (C_L, Z_t), which is consistent with the down milling mode. In the second situation, the radial depth of cut is negative, the raw material is on the left side of the local normal (O, Z). The raw material is also on the left side of the tool axis (C_L, Z_t) which induces an up milling mode. In the third situation, the raw material is still on the left side of the local normal (O, Z), as in 3-axis milling operation, and it implies an up milling mode. However, the raw material is on the right side of the tool axis (C_L, Z_t) and leads to a down milling mode. In conclusion, the milling mode is given by the position of the raw material relative to the plane (C_L, T, Z_t) which is driven by the tilt angle and radial depth of cut:

- if the raw material is located on the right of the plane (C_L, T, Z_t), then the mode is down milling,
- if the raw material is located on the left of the plane (C_L, T, Z_t), then the mode is up milling.

Table 1 gives effective cutting diameters of the 4 studied situations of Fig.7. The effective cutting diameters on the finished surface of the first three situations are the same. The finished surface is milled with only 2 teeth because the effective cutting diameters are less than Dz = 4.65 mm. The fourth situation is quite the same as situation 3 but with a 22° tilt angle. The 7° augmentation of the tilt angle leads to a generation of the finished surface with 4 teeth.

In conclusion of this 2nd section, a general analytical modeling of the milling cut of the 5-axis point milling is developed with the calculation method of the effective cutting diameters, the number of working teeth, and the determination of the milling mode. The cutting conditions with the tilt and lead angles are analytical parameters of the model and allow for the analysis of the cut and finished surfaces, the interaction between the tool and the raw material through the local cutting speed, the number of working teeth and the milling mode.

3. Analysis of Surface Topography

The previous section has established a geometrical model for the determination of the effective cutting diameters and the milling modes as local cutting conditions. The following will analyze the effects on the surface topography. 5 axis point milling presents a large number of geometrical configurations that exist and three main aspects are investigated: the milling mode, the cutting speed and the position of the cutter

location point. To study the effect of theses parameters on the surface roughness, various configuration are tested, but for all of them the number of working teeth is equal to four. Otherwise, the configurations with the cutter location point near the surface are situations with low cutting diameters and therefore have only 2 working teeth. This section presents the different configurations and starts with the topography observation and measurement methodology.

3.1. Experimental Context and Measure Methodology

The experimental evaluation is carried out using the following conditions. A Ti6Al4V part, having hardness around 33 HRc, is milled. Experimental tests were conducted with a 5 axis milling machine ZY\XBC (HSM 600U Mikron) without coolant. Unless otherwise stated, the cutting conditions are based on 0.12 mm/(tooth/rev) as feed per tooth f_z, 0.4 mm as radial depth of cut a_r and 0.3 mm as axial depth of cut a_a. The spindle speed *N* and the β_f lead and β_n tilt angles are the driving parameters of the study.

Measurements of the surface topography are reached using a white light interferometric microscope (Wyko NT1100 VEECO). The roughness parameters are calculated by the Vision software associated with the microscope. Two types of roughness criteria have been selected: surface roughness parameters (*Sa*, *St*, *Sq* and *Sz*) defined by ISO 25178-2 and roughness parameters from the bearing ratio analysis defined by ISO 13565 standard (*Spk*, *Sk, Svk, Mr1, Mr2, V1, V2*).

3.2. Cutting Edge Traces Synchronization

Figure 8 presents two observations of the same surface produced by several tool paths with the fixed cutting conditions: β_f = 45°, β_n = 0°, *N* = 3000 rpm. The error of

concentricity between the tool center O and the real rotation axis (about 10 µm) implies that the milled surface is obtained by only one tooth and not by 4 teeth. On the surface topography of both areas, a series of spherical cap marks is generated by the cutting edges trace, offset from the feed per revolution, in the feed direction, and the radial depth of cut in the perpendicular direction. The pattern difference between both areas is due to the synchronization (fig 8b) or not (fig 8a) between the first and the second horizontal tool paths. On Fig. 8a in the opposite phase, the step between both tool paths is equal to half the feed per revolution. The consequences on the surface and measures of roughness parameters are given in Table 2.

To impose a given and constant pattern along tool paths, it would be necessary to synchronize the angular position of the tool with the linear position of the cutter location point. This is not usual on CNC machine tools, even synchronization exists for rigid tapping operations where the angular position of the tool is linked to its axial position by the thread pitch. In the generation of complex sculptured surfaces, this synchronization is not proposed by industrial CNC.

In conclusion, the surface patterns and roughness parameters are modified by the synchronization of successive tool path. Consequently, milled surfaces are measured via the protocol set given above, on a range of 20 × 3.6 mm² (including 9 tool paths).

3.3. Influence of the Milling Mode

Usually, the down milling mode is often used for favoring a "better" surface quality. The following study is intended to illustrate the characteristics of the surface condition of the two modes.

Table 3 presents the different 5 axis milling configurations with a constant milling mode and a medium cutting speed equal to 80 m/min on the finished surface. Three possibilities of milling modes appear (up milling, down milling and combined up-down milling) on both surface types: cut and finished surfaces.

The surface measurement results of the various milling configurations show that configurations with the down milling mode promote a slight advantage over others. Nevertheless, morphological differences exist between these configurations and are identified by a multivariate Principal Components Analysis. This analysis considers the parameters measured on finished surfaces and cutting conditions as variables.

The main stages of a Principal Component Analysis (PCA) are:

- to calculate the linear correlation coefficients between the variables in pairs,
- to build the correlation matrix,
- to determine the eigenvalues and eigenvectors (called factors) of the correlation matrix,
- to project individuals on factors,
- to analyze the factors' meanings.

In the study of the influence of the milling mode on the surface topography, it is the 1st factor that shows the behavior difference between the two modes. Fig. 9 presents individuals (Table 3 data) positioned on the plane projection defined by factors 1 and 2 and the coefficients of the linear combination, which define the factors 1 and 2. For example, it appears that the 1st factor is strongly influenced by the variable "tilt angle" β_n. Similarly, the 2nd factor is labeled "radial depth of cut" a_r.

Thus, the 2nd factor is correlated with the variable radial depth of cut. Configurations 2 and 4 have a positive radial depth of cut and are on the same side of the 2nd factor. The 1st factor is strongly influenced by the tilt angle, and is actually a linear combination of input variables (decreasing in order of importance):

- Positive correlation: β_n … The increasing of the 1st factor induces an increasing of the parameter.
- Negative correlation: *Sz*, *St*, *Sq*, *Sa*, *V2*, *Svk*, *Spk*, *Sk*, *V1*… The increasing of the 1st factor induces a decreasing of these parameters.

Consequently the down milling mode (compared to the up milling mode) is characterized by a positive tilt angle and low roughness parameters like higher maximum high *St* (7.67 µm compare to 8.43 µm for up milling). However, the surface topology is different between the two modes. In the case of down milling mode, the reduced peak height *Spk* (0.99 µm compare to 1.13 µm for up milling), the core roughness depth *Sk* (3.52 µm compare to 3.70 µm), and the reduced valley depth *Svk* (0.63 µm compare to 0.70 µm), are lower. The volume *V2* that will retain lubricant or worn-out materials is lower in the case of the down milling mode with 16 nm compared to 19 nm for up milling mode.

A possible interpretation of these different observations is that the uncut chip thickness is increasing in the up milling mode. Thus, at the beginning of the chip forming on the finished surface, the thickness of the chip is very thin. The cut is not as good and generates protruding peaks and at least a greater maximum high *St*.

3.4. Influence of the Cutting Speed

The cutting speed is one of the cutting conditions that affects cutting the most, thus its influence is studied here in the following configuration: β_f = 0°, β_n = 75°, f_z = 0.12 mm/th/rev, a_r = -0.4 mm, a_a = 0.3 mm. Surfaces (20 × 3.6 mm²) were milled with medium cutting speeds on the finished surface between 5, 10, 15, 20, 30, 40 and 50 m/min. This configuration produces a variation of effective diameters on the finished surface of 1.8% ($D_{eff\ min\ Finished\ Surf}$ = 11.48 mm & $D_{eff\ max\ Finished\ Surf}$ = 11.69 mm then Z = 4). This variation is the same on the cutting speed along the cutting edge. It is assumed it has a negligible effect on the surface quality.

The analysis of measured roughness parameters is carried out with the Principal Component Analysis. The first factor is the most interesting. The 1st factor on Fig. 10 shows the decreasing cutting speed of 7 surfaces made. There are two groups of cutting speed: those lower or equal to 30 m/min (on the right side) and those above (on the left one). The 1st factor is influenced with a positive correlation to volume *V2*, reduced valley depth *Svk*, material ratio of reduced peak height *Mr1*, and a negative correlation to core roughness depth *Sk*, material ratio of reduced valley depth *Mr2*, roughness *Sa* and *Sq*. Therefore, low cutting speeds induce larger volumes *V2* (18 nm compare to 9 nm in the case of high cutting speed), higher reduced valley depths *Svk* (0.70 µm compare to 0.50 µm), larger material ratios of reduced peak height *Mr1* (9 % compare to 7 %), and shorter core roughness depths *Sk* (3.7 µm compare to 4.3 µm), smaller material ratios of reduced valley depth *Mr2* (95 % compare to 96.5 %), lower roughness values *Sa* (1.04 µm compare to 1.16 µm).

The case of very low cutting speeds (i.e. 5 m/min) is situated at the top of the 1st and 2nd factors. The associated profile is characterized by a higher *Svk* and *Spk* and a larger volume *V2,* which will retain lubricant or worn-out materials. One possible explanation is that the cutting edges at a lower speed tear out the chips and create more valleys and peaks.

In conclusion, the influence of cutting speed on the surface is in accordance with the recommended minimum cutting speed of 30 m/min. The surface topography is consistent with the cutting behavior given by the specific energy (not developed here). Low cutting speeds generate higher specific energies and more valleys and peaks.

3.5. Influence of the cutter location point

The cutting speed of the cutter location point C_L is null. On a real tool, an area of the edge tries to cut the raw material with a very low cutting speed. The originality of this study is to analyze the influence of the cutter location point on the surface roughness and to keep constant the influences of the cutting speed, the milling mode and the number of working teeth on the finished surface. The objective is to achieve surfaces obtained with a constant medium cutting speed on the finished surface. Cutting conditions of the 8 configurations used are detailed in Table 4 and lead to 2 working teeth. Each orientation of the tool axis is tested with the two milling modes.

Configurations 5 and 6 (Fig. 11) have the tool axis normal to the finished surface. So, the cutter location point is positioned on the finished surface border. The maximum effective diameter of the finished surface is the smallest of all the configurations and defines the cutting speed range on the finished surface. The spindle speed of the machine is limited to 24 000 rpm, which implies a medium cutting speed fixed to

15 m/min for all configurations. Thus the attempted cutting speed of 30 m/min cannot be reached.

For different configurations, the cutter location point is positioned relative to the finished and cut surfaces:

- in the center of the finished surface for configurations 7 and 8,
- at the border of the cut surface but outside the finished surface for configurations 9 and 10,
- outside of the cut surface but close to and within the effective diameter below 4.65 mm to remain in the work area with 2 working teeth, for configurations 11 and 12.

The 8 configurations (5 to 12) were performed then measured according to the same protocol, and exploited using a Principal Component Analysis. The 1^{st} and 2^{nd} factors of the PCA (Fig. 12) provide a good summary of the differences between surface topographies.

The 1^{st} factor shows a clear contrast between the configurations where the cutter location point is in contact with the finished surface (configuration 5 to 8) and those outside thereof (configuration 9 to 12). The greater the value of the 1^{st} factor (Fig. 12) is:

- the greater the volume of retained lubricant or worn-out materials *V2* is,
- the greater the reduced valley depth *Svk* is,
- the lesser the other parameters are (in decreasing order of importance): *Spk*, *V1*, *Sk*, *Mr1*, *Sa*, *Sq*...

Therefore configurations 5 to 8, in which the cutter location point is in contact with the finished surface (compared to configurations without contact with the finished surface), present a volume of retained lubricant *V2* of 120 nm (compare to 18 nm), a reduced valley depth *Svk* of 1.33 µm (compare to 0.60 µm), a reduced peak height *Spk* of 0.59 µm (compare to 1.27 µm), a volume of reduced peak height *V1* of 0.02 µm (compare to 0.12 µm), a core roughness depth *Sk* of 2.11 µm (compare to 3.19 µm) and a *Sa* roughness of 0.74 µm (compare to 1.06 µm)…

The 2nd factor shows (Fig. 12) the contrast between configurations 5 and 6 where the cutter location point is situated on the finished surface border and configurations 7 and 8 where the cutter location point is positioned in the finished surface. The 2nd factor is characterized with:

- a reduced valley depth *Svk* high,
- an important volume of retained lubricant or worn-out materials *V2*,
- high levels of roughness parameters *St* and *Sz*,
- low material ratios of reduced valley depth *Mr2* and peak height *Mr1*.

These observations can be understood with three explanations. The first one is kinematic. These phenomena can be due to the cutting velocity gradient which is increasing with the 1st factor. If the velocity gradient is low, all points of the cutting edge present similar cutting behavior and the geometry of the finished surface is close to a circular profile (cf. Fig. 13). Conversely, an important gradient of cutting velocity along the cutting edge induces an important variation of the cutting behavior. Then, specific energy and peak profiles are affected.

The second reason is related to the cutting continuity because if the cutter location point is away from the finished surface and the cut surface, then the cutting continuity is lower. A cutting edge is coming into the material after the preceding is leaving the material, which produces a sharp variation in the cutting edge. In the case of configurations 7 and 8, the cutter location point is situated on the finished surface and thus there is cutting continuity. So, cutting forces are probably more continuous and progressive. It is possible that the radial forces in certain angular positions of the tool are balanced and the radial deflection of the tool is reduced. If the ball end mill is constantly in contact with the material, then it improves the damping effect on the cutting dynamic and thus promotes a greater stability.

The third reason is geometric. The presence of the cutter location point on the finished surface border means that this is directly involved in the generation of the surface. If the cutter location point is in contact with the material but out of the border (for example the configurations 7 and 8), then this point does not contribute to the generation of the finished surface.

In conclusion, the surface topography generated on the finished surface is related to the position of the cutter location point. The configuration placing the cutter location point in the centre of the finished surface implies a better quality surface but requires an accurate control of the tool axis position relative to the cutting area. Nevertheless, it is also necessary to investigate the effect on the tool wear.

4. Conclusions

This study proposes a geometrical model to evaluate the local cutting conditions for 5 axis point milling using a ball end mill. This fully analytical model proposes:

- a calculation method for the effective cutting diameters on cut and finished surfaces,
- the identification of the number of working teeth,
- the determination of the milling modes on cut and finished surfaces.

An experimental surface roughness analysis allows for the observation of the effect of the milling mode, the cutting speed and the cutter location point. The titanium alloy behaves such that the down milling mode has a slight advantage on average roughness parameters. However, the cutting speed modifies the surface topography and two different behaviors are developed depending on whether the cutting speed is lower or greater than 30 m/min. Finally, configurations with small effective diameters are possible by controlling the position of the cutter location point relative to the finished surface. Surface topography is optimum for configurations where the cutter location point is situated in the middle of the finished surface.

Further work would consider the development of a geometrical model during 5 axis milling of curved surfaces.

References

[1] Boyer, R. R., 1996, “An overview on the use of titanium in the aerospace industry,” Int. Symp. Metall. Technol. Titan. Alloys, **213**(1-2), pp. 103–114.

[2] Corduan, N., Himbert, T., Poulachon, G., Dessoly, M., Lambertin, M., Vigneau, J., and Payoux, B., 2003, “Wear mechanisms of new tool materials for Ti-6Al-4V high performance machining,” CIRP Ann. - Manuf. Technol., **52**(1), pp. 73–76.

[3] Kim, K.-K., Kang, M.-C., Kim, J.-S., Jung, Y.-H., and Kim, N.-K., 2002, “A study on the precision machinability of ball end milling by cutting speed optimization,” J. Mater. Process. Technol., **130-131**, pp. 357–362.

[4] Fan, J., 2014, “Cutting speed modelling in ball nose milling applications,” Int. J. Adv. Manuf. Technol.

[5] Boujelbene, M., Moisan, A., Bouzid, W., and Torbaty, S., 2007, “Variation cutting speed on the five axis milling,” J. Achiev. Mater. Manuf. Eng., **21**(2), pp. 7–14.

[6] Daymi, A., Boujelbene, M., Ben Amara, A., and Linares, J. M., 2009, “Improvement of the surface quality of the medical prostheses in high speed milling,” Int. Rev. Mech. Eng., **3**(5), pp. 566–572.

[7] Ozturk, B., and Lazoglu, I., 2006, “Machining of free-form surfaces. Part I: Analytical chip load,” Int. J. Mach. Tools Manuf., **46**(7-8), pp. 728–735.

[8] Prat, D., Fromentin, G., Poulachon, G., and Duc, E., 2012, “Experimental Analysis and Geometrical Modeling of Cutting Conditions Effect in 5 Axis Milling with Ti6Al4 V Alloy,” Procedia CIRP, **1**, pp. 84–89.

[9] Ozturk, E., Tunc, L. T., and Budak, E., 2009, “Investigation of lead and tilt angle effects in 5-axis ball-end milling processes,” Int. J. Mach. Tools Manuf., **49**(14), pp. 1053–1062.

[10] Lin, R.-S., and Koren, Y., 1996, “Efficient tool-path planning for machining free-form surfaces,” ASME J. Eng. Ind., **118**(1), pp. 20–27.

[11] Imani, B. M., and Elbestawi, M. A., 2001, “Geometric Simulation of Ball-End Milling Operations,” ASME J. Manuf. Sci. Eng., **123**(2), p. 177.

[12] Bailey, T., Elbestawi, M. A., El-Wardany, T. I., and Fitzpatrick, P., 2002, “Generic Simulation Approach for Multi-Axis Machining, Part 1: Modeling Methodology,” ASME J. Manuf. Sci. Eng., **124**(3), p. 624.

[13] Bouzakis, K.-D., Aichouh, P., and Efstathiou, K., 2003, “Determination of the chip geometry, cutting force and roughness in free form surfaces finishing milling, with ball end tools,” Int. J. Mach. Tools Manuf., **43**(5), pp. 499–514.

[14] Lavernhe, S., Quinsat, Y., and Lartigue, C., 2010, “Model for the prediction of 3D surface topography in 5-axis milling,” Int. J. Adv. Manuf. Technol., **51**(9-12), pp. 915–924.

[15] Quinsat, Y., Lavernhe, S., and Lartigue, C., 2011, “Characterization of 3D surface topography in 5-axis milling,” Wear, **271**(3-4), pp. 590–595.

[16] Lavernhe, S., Quinsat, Y., Lartigue, C., and Brown, C., 2014, “Realistic simulation of surface defects in five-axis milling using the measured geometry of the tool,” Int. J. Adv. Manuf. Technol.

[17] Liu, X., Soshi, M., Sahasrabudhe, A., Yamazaki, K., and Mori, M., 2006, “A geometrical simulation system of ball end finish milling process and its application

for the prediction of surface micro features," ASME J. Manuf. Sci. Eng., **128**(1), pp. 74–85.

[18] Buj-Corral, I., Vivancos-Calvet, J., and Domínguez-Fernández, A., 2012, "Surface topography in ball-end milling processes as a function of feed per tooth and radial depth of cut," Int. J. Mach. Tools Manuf., **53**(1), pp. 151–159.

[19] Zeroudi, N., and Fontaine, M., 2012, "Prediction of machined surface geometry based on analytical modelling of ball-end milling," Procedia CIRP, **1**, pp. 108–113.

[20] Denkena, B., Böß, V., Nespor, D., and Samp, A., 2011, "Kinematic and stochastic surface topography of machined tial6v4-parts by means of ball nose end milling," Procedia Engineering, pp. 81–87.

[21] Zhang, W.-H., Tan, G., Wan, M., Gao, T., and Bassir, D. H., 2008, "A New Algorithm for the Numerical Simulation of Machined Surface Topography in Multiaxis Ball-End Milling," ASME J. Manuf. Sci. Eng., **130**(1), p. 011003.

[22] Han, S. G., and Zhao, J., 2010, "Effect of tool inclination angle on surface quality in 5-axis ball-end milling," 2009 Int. Conf. Manuf. Sci. Eng. ICMSE 2009, **97-101**, pp. 2080–2084.

[23] Chen, X., Zhao, J., Dong, Y., Han, S., Li, A., and Wang, D., 2013, "Effects of inclination angles on geometrical features of machined surface in five-axis milling," Int. J. Adv. Manuf. Technol., **65**(9-12), pp. 1721–1733.

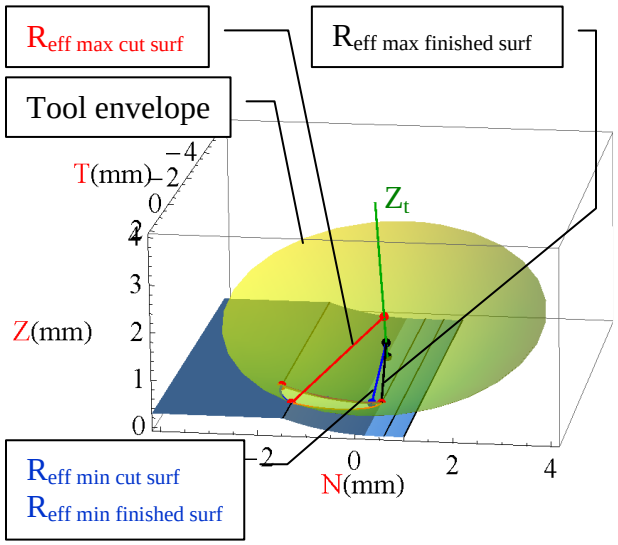

Fig. 1 Effective cutting radius on the cut and finished surface (β_f = 20°, β_n = 0°, a_r = 0.4 mm, a_a = 0.3 mm)

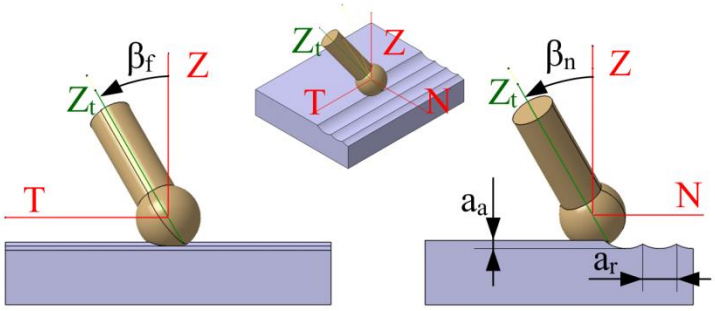

Fig. 2 Definition of the β_f lead and β_n tilt angles and a_a axial and a_r radial depth of cut

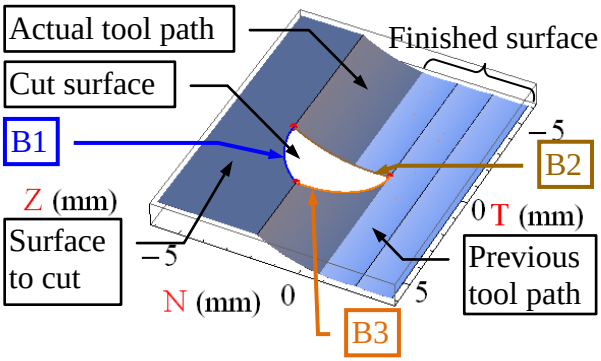

Fig. 3 Machined part with the cut and finished surfaces

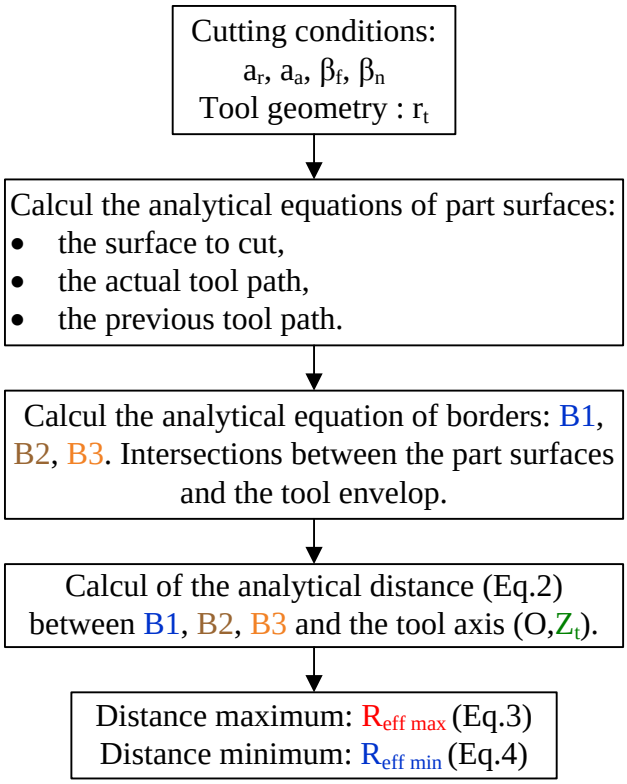

Fig. 4 Algorithm for the computation of effective cutting radius

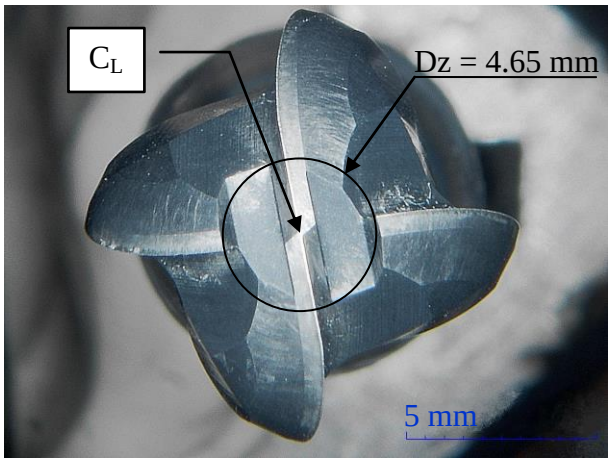

Fig. 5 Geometry of the ball end mill cutter used in the study

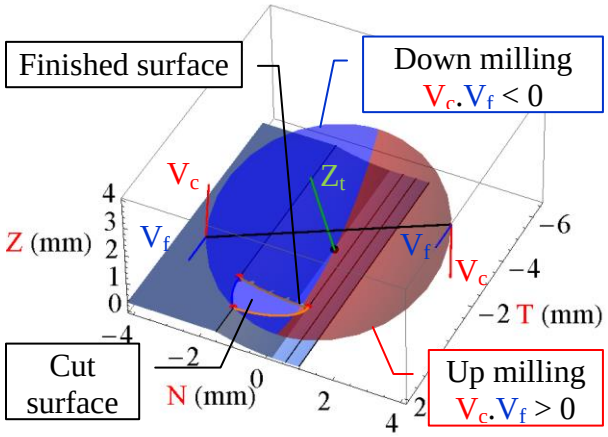

Fig. 6 Milling mode for the configuration (β_f = 20°, β_n = 0°, a_r = 0.4 mm, a_a = 0.3 mm)

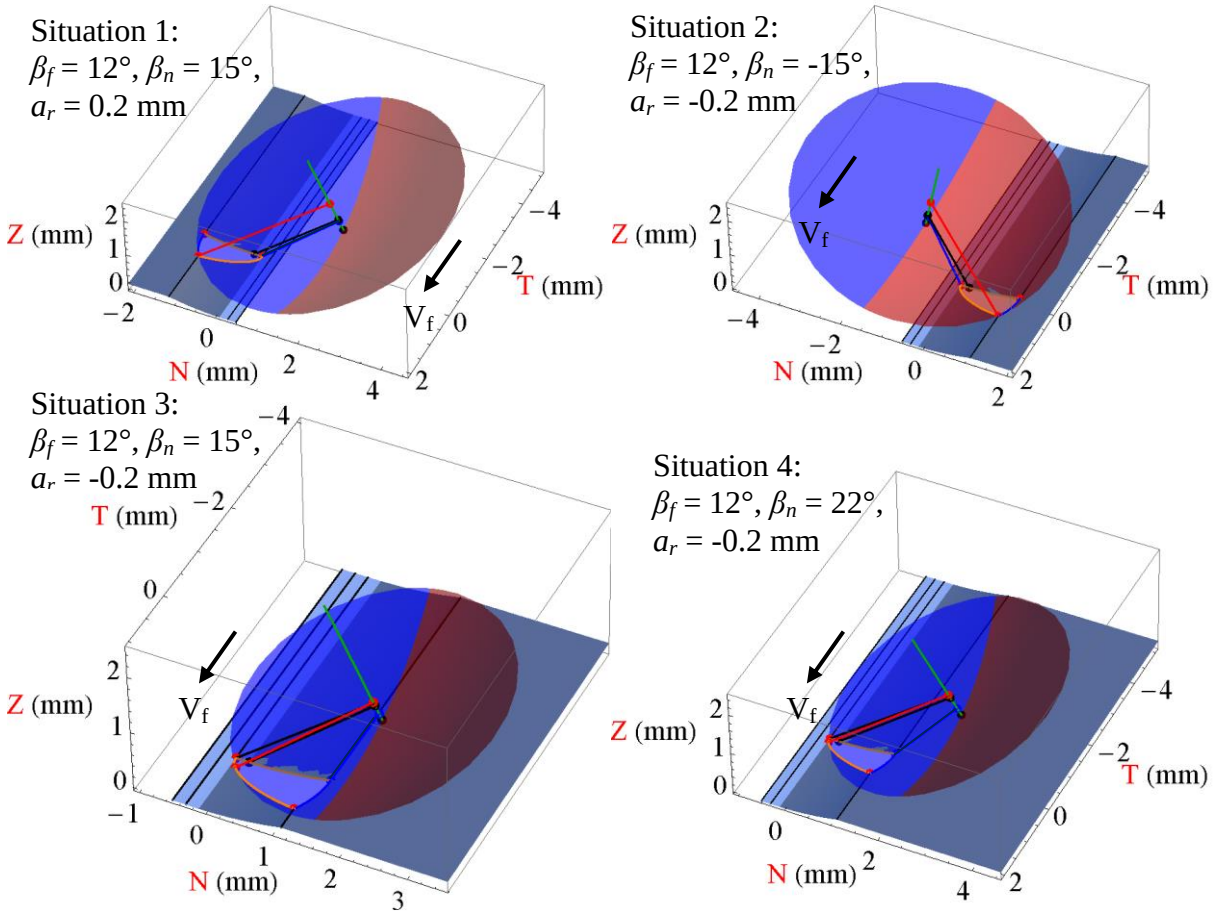

Fig. 7 Effective cutting radius and milling modes of 4 situations (a_a = 0.15 mm)

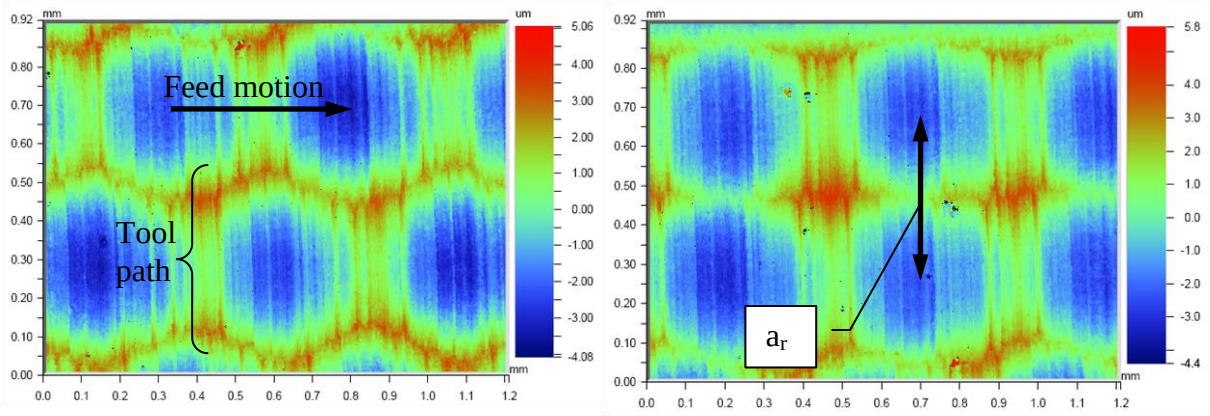

a) Area with 2 paths in opposite phase b) Area with 2 paths traces in phase

Fig. 8 Surface topography of two different areas of the same surface (β_f = 45°, β_n = 0°, N = 3000 rpm, f_z = 0.12 mm/th/rev, a_r = 0.4 mm, a_a = 0.3 mm)

Factor	1	2
a_r	0.10	0.49
β_n	0.28	-0.09
St	-0.34	-0.07
Mr1	-0.19	0.42
Mr2	0.07	-0.49
Sk	-0.27	-0.32
Spk	-0.28	0.23
Svk	-0.31	-0.20
V1	-0.25	0.32
V2	-0.32	0.09
Sa	-0.33	-0.13
Sq	-0.34	-0.09
Sz	-0.35	-0.05

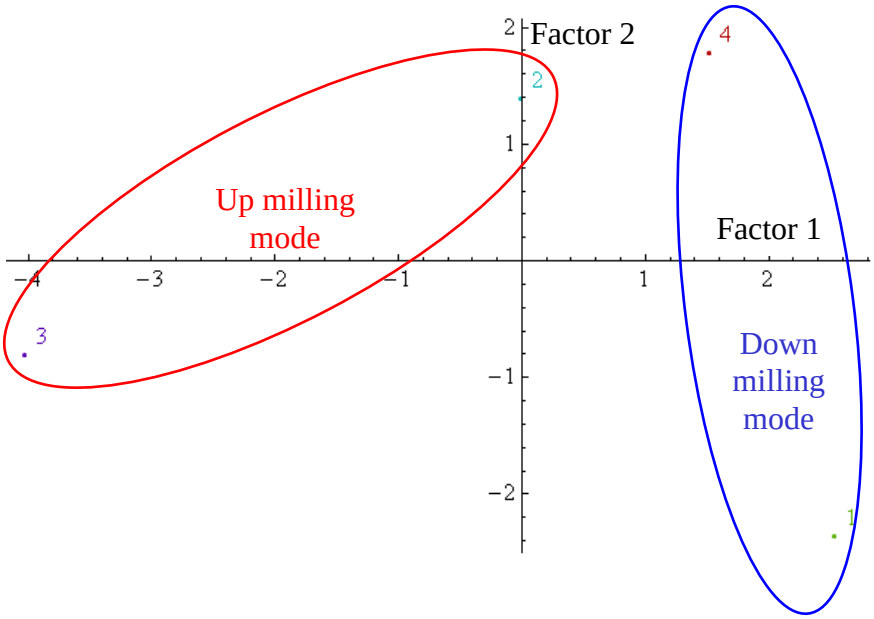

Fig. 9 Projection of individuals on the 1st and 2nd factor to study the influence of the milling mode

Factor	1	2
V_c	-0.313	-0.263
St	0.031	-0.492
Mr1	0.302	-0.216
Mr2	-0.347	-0.079
Sk	-0.350	0.031
Spk	0.168	-0.457
Svk	0.326	0.141
V1	0.287	-0.275
V2	0.333	0.177
Sa	-0.347	-0.033
Sq	-0.344	-0.013
Sz	-0.030	-0.546

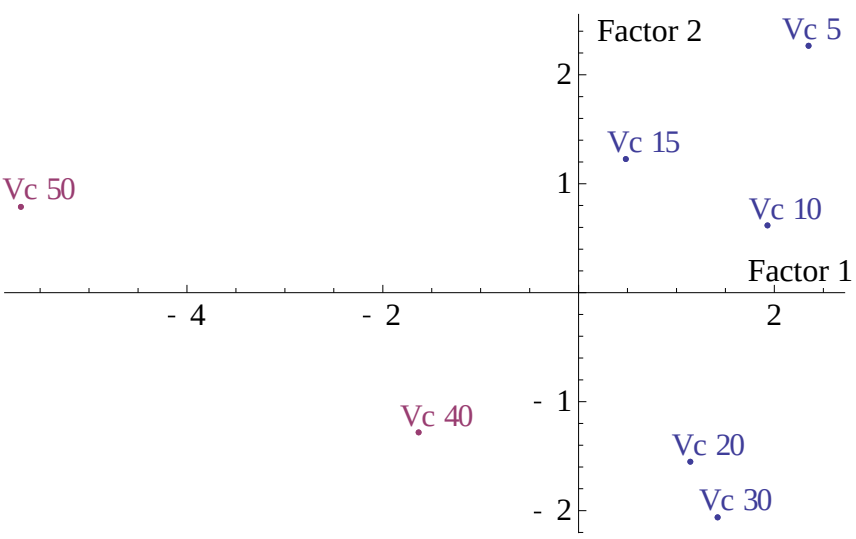

Fig. 10 Projection of individuals on the 1st and 2nd factors to study the influence of the cutting speed

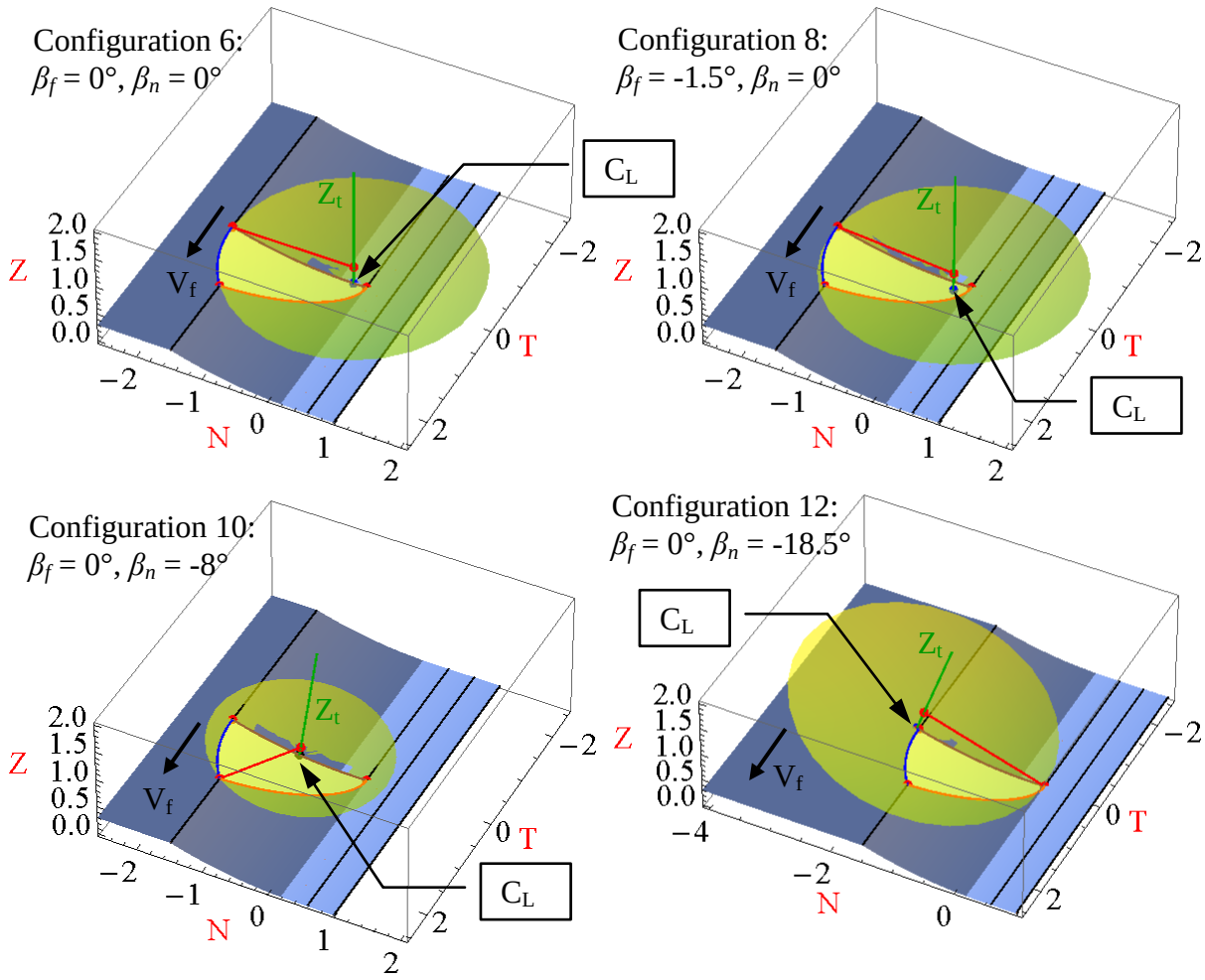

Fig. 11 Representation of configurations to study the influence of the cutter location point position (a_r = 0.4 mm, a_a = 0.3 mm)

Factor	1	2
St	-0.210	0.393
Mr1	-0.367	-0.102
Mr2	-0.242	-0.395
Sk	-0.370	-0.020
Spk	-0.384	-0.047
Svk	0.196	0.436
V1	-0.375	-0.042
V2	0.222	0.410
Sa	-0.325	0.254
Sq	-0.297	0.316
Sz	-0.236	0.390

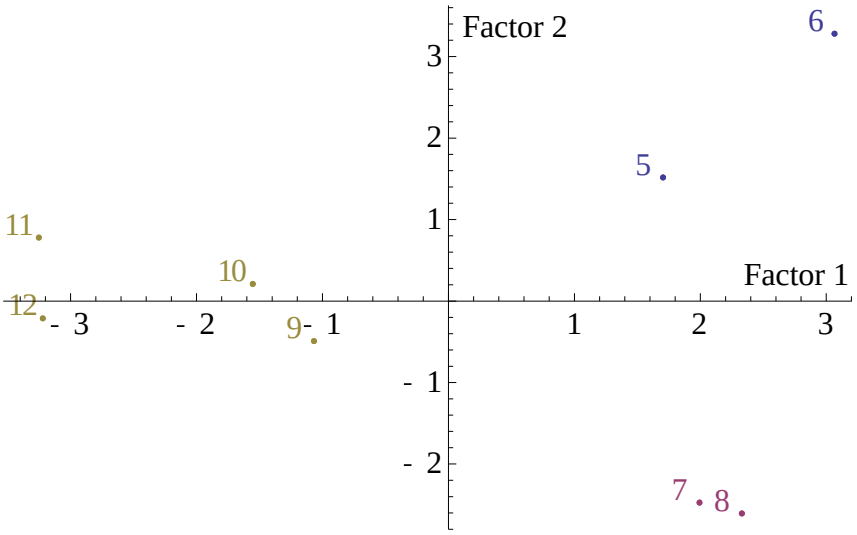

Fig. 12 Projection of individuals on the factors 1 and 2 to study the influence of the cutter location point position

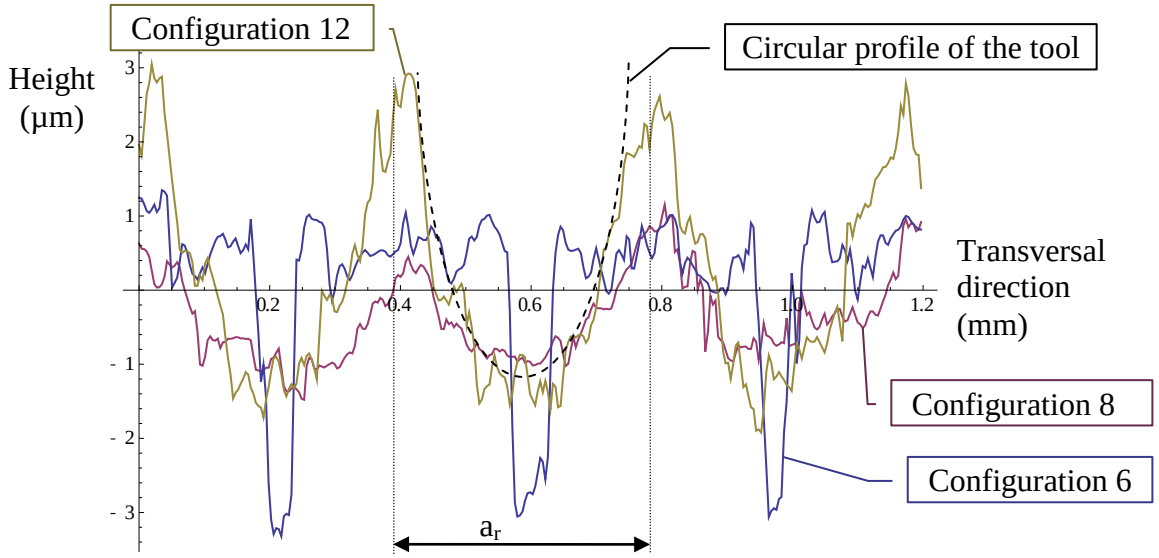

Fig. 13 Transversal profile of configuration 6, 8 and 12

Table 1
Effective cutting diameters of the 4 situations and consequences on the number of working teeth

Situation	1	2	3	4
$D_{eff\ min\ cut\ surf}$ (mm)	3.74	3.74	2.45	2.98
$D_{eff\ max\ cut\ surf}$ (mm)	6.3	6.3	4.13	5.19
$D_{eff\ min\ finished\ surf}$ (mm)	3.74	3.74	3.74	4.82
$D_{eff\ max\ finished\ surf}$ (mm)	4.03	4.03	4.03	5.14
number of working teeth on finished surface	2	2	2	4

Table 2
Roughness parameters measured on the two zones of Fig. 8

	opposite phase	in phase
Sa (µm)	1.24	1.23
St (µm)	9.14	10.16

Table 3
Cutting conditions for the milling modes tests (N = 3000 rpm, f_z = 0.12 mm/th/rev and a_a = 0.3 mm)

Configuration	1	2	3	4
β_f (°)	44.7	44.7	44.7	44.7
β_n (°)	8	-8	-8	8
a_r (mm)	-0.4	0.4	-0.4	0.4
$D_{eff\ min\ Finish\ Surf}$ (mm)	8.45	8.45	8.45	8.45
V_c (m/min) for $D_{eff\ min\ Finished\ Surf}$	79.62	79.62	79.62	79.62
$D_{eff\ max\ Finish\ Surf}$ (mm)	8.53	8.53	8.53	8.53
V_c (m/min) for $D_{eff\ max\ Finished\ Surf}$	80.37	80.37	80.37	80.37
Milling mode on finished surface	down	up	up	down
Milling mode on cut surface	up-down	up-down	up	down

Table 4
Cutting conditions to study the influence of the cutter location point (a_a = 0.3 mm)

Configuration	5	6	7	8	9	10	11	12
β_f (°)	0	0	-1.5	-1.5	0	0	0	0
β_n (°)	0	0	0	0	8	-8	18.5	-18.5
N (rpm)	24000	24000	16000	16000	3000	3000	1300	1300
a_r (mm)	-0.4	0.4	-0.4	0.4	-0.4	0.4	-0.4	0.4
$D_{eff\ min}$ (mm)	0	0	0	0	0	0	0.06	0.06
V_c (m/min) for $D_{eff\ min}$	0	0	0	0	0	0	0.26	0.26
$D_{eff\ max}$ (mm)	3.75	3.75	3.76	3.76	2.67	2.67	4.18	4.18
V_c (m/min) for $D_{eff\ max}$	35.3	35.3	35.3	35.3	25.2	25.2	17.1	17.1
$D_{eff\ min\ Finished\ Surf}$ (mm)	0.000	0.000	0.09	0.09	1.27	1.27	3.43	3.43
V_c (m/min) for $D_{eff\ min\ Finished\ Surf}$	0.0	0.0	4.3	4.3	12.0	12.0	14.0	14.0
$D_{eff\ max\ Finished\ Surf}$ (mm)	0.4	0.4	0.51	0.51	2.07	2.07	4.19	4.19
V_c (m/min) for $D_{eff\ max\ Finished\ Surf}$	30.2	30.2	25.6	25.6	19.5	19.5	17.1	17.1